

Europium Pyridinethiolates: Synthesis, Structure, and Thermolysis

M. Berardini and J. Brennan*

Department of Chemistry, Rutgers, The State University of New Jersey, Piscataway, New Jersey 08855-0939

Received March 17, 1995[⊗]

The transmetalation reaction of $\text{Hg}(\text{SPy})_2$ ($\text{SPy} = \text{S}-2\text{-NC}_5\text{H}_4$) with Eu in pyridine gives the europium(II) pyridinethiolate coordination complex $(\text{py})_4\text{Eu}(\text{SPy})_2$ (**1**) in 96% isolated yield. The reaction of **1** with BIPY in THF results in displacement of the pyridine ligands and the formation of the divalent coordination complex $(\text{BIPY})_2(\text{THF})_2\text{Eu}(\text{SPy})_2$ (**2**). Low-temperature single-crystal X-ray diffraction experiments show that **1** and **2** are molecular 8 coordinate compounds. They are both intensely colored due to the presence of a visible europium-to-pyridine or europium-to-BIPY charge transfer (CT) absorption band. Trivalent $[\text{PEt}_4][\text{Eu}(\text{SPy})_4]$ (**3**) was prepared from the reaction of Eu/Hg amalgam with PySSPy in the presence of $[\text{PEt}_4][\text{SPy}]$. X-ray diffraction analysis of **3** shows that all the pyridinechalcogenolate ligands are chelating the Eu(III) ion and there are three different eight coordinate isomers within the unit cell. Compound **3** is intensely colored because of a visible S-to-Eu CT absorption. At 500 °C, **3** decomposes to give EuS and a mixture of PySSPy , PySPy , EtSPy , and SPeEt_3 . Crystal data (Mo $K\alpha$, 153(5) K): **1**, orthorhombic space group $Pna2_1$, $a = 19.006(2)$ Å, $b = 9.724(5)$ Å, $c = 15.592(5)$ Å, $Z = 4$; **2**, monoclinic space group Cc , $a = 9.851(2)$ Å, $b = 16.817(3)$ Å, $c = 17.271(2)$ Å, $\beta = 92.67(2)^\circ$, $Z = 4$; **3**, monoclinic space group $P2_1/n$, $a = 15.043(3)$ Å, $b = 16.036(6)$ Å, $c = 26.444(5)$ Å, $\beta = 90.54(2)^\circ$, $Z = 4$.

Introduction

There are both fundamental and applied motivations for studying the coordination chemistry of the lanthanide ions bound to anionic thiolate, selenolate, or telluroolate (chalcogenolate) ligands. The nature of the bonding between these electropositive metal ions and the heavier, less electronegative chalcogenolates is relatively unexplored. While bonding in the solid state lanthanide chalcogenolate compounds has long been discussed in terms of considerable covalent bonding character,¹ little is known about the nature of molecular compounds containing lanthanide–chalcogen bonds.² In the past few years there has been a surge of interest in preparing lanthanide complexes with chalcogenolates as the only anions³ because of their possible use as lanthanide doping sources in semiconductor⁴ as well as non-oxide-based fiber optic technology.⁵

There are two advantages of using molecular lanthanide chalcogenolates as doping sources. First, molecular chalcogenolates decompose to deliver LnE_x . The resultant lanthanide coordination sphere in the chalcogenide matrix contains only one type of chalcogen atom that gives optimally sharp optical properties. More importantly, the lanthanide is directly bound

to the chalcogen matrix. Second, molecular lanthanide chalcogenolates may be used to deliver uniform concentrations of Ln ions at relatively low temperatures. Lanthanide tellurolates decompose below 100 °C, and the thiolates decompose below 400 °C. Low temperatures are important when the desired product is a metastable solid (i.e. a fiber optic glass, which may crystallize at elevated temperatures). For both reasons, molecular chalcogenolate complexes are attractive Ln sources, especially in comparison with conventional lanthanide halide or carboxylate sources.

The chalcogenolate chemistry of Eu has attracted a disproportionate share of attention from synthetic inorganic chemists^{3e,f,h,j-1} because Eu is redox active and because Eu will emit red photons in electroluminescent devices.^{4j-1} Given the extensive literature describing europium(II) chalcogenolates and the complete absence of related europium(III) chalcogenolate complexes, it is clear that there is an inherent inability of chalcogenolates to stabilize electropositive metals in higher oxidation states (particularly with Eu(II), which has a half-filled

[⊗] Abstract published in *Advance ACS Abstracts*, November 1, 1995.

- (1) (a) Gerth, G.; Kienle, P.; Luchner, K. *Phys. Lett. A* **1968**, *27*, 557–8. (b) Eatough, N. L.; Hall, H. T. *Inorg. Chem.* **1970**, *9*, 417–8. (c) Dagys, R. S.; Anisimov, F. G. *Sov. Phys. Solid State* **1984**, *26*, 547–8. (d) Wachter, P. *Crit. Rev. Solid State* **1972**, *3*, 189–241. (e) Byrom, E.; Ellis, D. E.; Freeman, A. J. *Phys. Rev. B* **1976**, *14*, 3558–68. (f) Zhukov, V. P.; Gubanov, V. A.; Weber, J. J. *Chem. Phys. Solids* **1981**, *42*, 631–9. (2) (a) Schumann, H.; Albrecht, I.; Hahn, E. *Angew. Chem. Int. Ed. Engl.* **1985**, *24*, 985–6. (b) Berg, D.; Burns, C.; Andersen, R. A.; Zalkin, A. *Organometallics* **1988**, *7*, 1858–63. (c) Berg, D. J.; Burns, C.; Andersen, R. A.; Zalkin, A. *Organometallics* **1989**, *8*, 1865–70. (d) Zalkin, A.; Berg, D. J. *Acta Crystallogr.* **1988**, *44C*, 1488–9. (e) Evans, W.; Grate, J. W.; Bloom, I.; Hunter, W. E.; Atwood, J. L. *J. Am. Chem. Soc.* **1985**, *107*, 405–9. (f) Evans, W.; Rabe, G.; Ziller, J.; Doedens, R. *Inorg. Chem.* **1994**, *33*, 2719–26. (g) Welder, M.; Noltmeyer, M.; Pieper, U.; Schmidt, H.; Stalke, D.; Edelmann, F. *Angew. Chem., Int. Ed. Engl.* **1990**, *29*, 894–6. (h) Wedler, M.; Recknagel, A.; Gilje, J. W.; Nottemeyer, M.; Edelmann, F. T. J. *Organomet. Chem.* **1992**, *426*, 295.

- (3) (a) Cetinkaya, B.; Hitchcock, P. B.; Lappert, M. F.; Smith, R. G. *J. Chem. Soc., Chem. Commun.* **1992**, 932–3. (b) Strzelecki, A. R.; Timinski, P. A.; Hesel, B. A.; Bianconi, P. A. *J. Am. Chem. Soc.* **1992**, *114*, 3159–60. (c) Cary, D. R.; Arnold, J. J. *Am. Chem. Soc.* **1993**, *115*, 2520–1. (d) Berardini, M.; Emge, T.; Brennan, J. G. *J. Chem. Soc., Chem. Commun.* **1993**, 1537–8. (e) Berardini, M.; Emge, T.; Brennan, J. G. *J. Am. Chem. Soc.* **1993**, *115*, 8501–2. (f) Khasnis, D. V.; Lee, J.; Brewer, M.; Emge, T. J.; Brennan, J. G. *J. Am. Chem. Soc.* **1994**, *116*, 7129–33. (g) Brewer, M.; Khasnis, D.; Buretea, M.; Berardini, M.; Emge, T. J.; Brennan, J. G. *Inorg. Chem.* **1994**, *33*, 2743–7. (h) Carey, D. R.; Arnold, J. *Inorg. Chem.* **1994**, *33*, 1791–5. (i) Mashima, K.; Nakayama, Y.; Kanehisa, N.; Kai, Y.; Nakamura, A. *J. Chem. Soc., Chem. Commun.* **1993**, 1847–8. (j) Strzelecki, A. R.; Likar, C.; Hesel, B. A.; Utz, T.; Lin, M. C.; Bianconi, P. A. *Inorg. Chem.* **1994**, *33*, 5188–94. (k) Mashima, K.; Nakayama, Y.; Fukumoto, H.; Kanehisa, N.; Kai, Y.; Nakamura, A. *J. Chem. Soc., Chem. Commun.* **1994**, 2523–4. (l) Berardini, M.; Emge, T. J.; Brennan, J. G. *J. Am. Chem. Soc.* **1994**, *116*, 6941–2. (m) Lee, J.; Brewer, M.; Berardini, M.; Brennan, J. *Inorg. Chem.* **1995**, *34*, 3215–20. (n) Berardini, M.; Emge, T.; Brennan, J. *Inorg. Chem.* **1995**, *34*, 5327–34. (o) Carey, D.; Ball, G. E.; Arnold, J. *J. Am. Chem. Soc.* **1995**, *117*, 3492. (p) Gharia, K. S.; Singh, M.; Mathur, S.; Roy, R.; Sankhla, B. S. *Synth. React. Inorg. Met.-Org. Chem.* **1982**, *12*, 337–45.

f^7 valence shell). Arenethiolate ligands appear to form only divalent $\text{Eu}(\text{SR})_2$ coordination complexes that do not react further with diaryl disulfide.^{3k} The europium(III) dithiocarbamates^{6ab} and dithiophosphonates^{6c,d} are proof that, with adequate resonance stabilization, sulfur-based anions are capable of stabilizing $\text{Eu}(\text{III})$. Still, the intense red color of these compounds is due to a relatively low-energy S-to-Eu charge transfer absorption band that suggests the $\text{Eu}(\text{III})$ oxidation state is not particularly stable. The well documented use of the pyridinethiolate ligand (S-2-NC₅H₄ or SPy) to form stable complexes with transition metals,⁷ and in particular the ability of this thiolate to form stable complexes with $\text{Ti}(\text{III})$,⁷ⁿ $\text{Rh}(\text{III})$,^{7f} and $\text{Pt}(\text{III})$,^{7a} led us to examine pyridinethiolate coordination to the lanthanide elements. This paper demonstrates how the resonance-stabilized chelating pyridine-2-thiolate ligand can be used to stabilize $\text{Eu}(\text{II})$ and $\text{Eu}(\text{III})$ compounds. The structural and optical properties of both europium(II) and europium(III) pyridine thiolate complexes are described, and the trivalent complex thermolysis product is identified.

Experimental Section

General. All syntheses were carried out under ultrapure nitrogen (JWS), using conventional drybox or Schlenk techniques. THF and pyridine (Fisher) were refluxed continuously over K and KOH, respectively, and collected immediately prior to use. Dipyridinyl disulfide and mercaptopyridine were purchased from Aldrich and Strem. $\text{Hg}(\text{S}-2\text{-NC}_5\text{H}_4)_2$ was prepared according to the literature procedure.⁷ⁱ Eu and Hg were purchased from Strem. Melting points were taken in sealed capillaries and are uncorrected. IR spectra were taken on a Mattus Cygnus 100 FTIR spectrometer and recorded from 4000 to 450 cm^{-1} as a Nujol mull. Electronic spectra were recorded on a Varian DMS 100S spectrometer with the samples in a 0.10 mm quartz cell attached to a Teflon stopcock. Elemental analyses were performed by Quantitative Technologies, Inc. (Salem, NJ). NMR spectra were obtained on either a Varian Gemini 300 MHz or a Varian 400 MHz NMR spectrometer and are reported in δ (ppm). The powder diffraction pattern was obtained with a SCINTAG PAD V diffractometer (Cu K α radiation).

(py)₄Eu(S-2-C₅H₄N)₂ (1). Eu (1.2 g, 8.0 mmol) and Hg(S-2-C₅H₄N)₂ (3.2 g, 7.6 mmol) were added to pyridine (50 mL), and the

mixture was stirred for 48 h. The deep orange solution was filtered and concentrated to 10 mL, upon which an orange precipitate formed. The precipitate was redissolved by heating the solution, and upon subsequent cooling, deep orange crystals began to form within minutes. After a day the solution was cooled (-20°C) to give **1** (5.0 g, 96%). Complex **1** does not melt below 300°C but appears to lose pyridine rapidly at 65°C and turns bright orange between 150 and 160°C . Upon isolation the compound rapidly loses one pyridine donor at room temperature. Anal. Calcd for C₂₅H₂₃N₅EuS₂: C, 49.3; H, 3.81; N, 11.5. Found: C, 49.3; H, 3.87; N, 11.4. IR: 2923 (s), 2855 (s), 1613 (w), 1577 (w), 1532 (w), 1462 (s), 1446 (s), 1405 (m), 1378 (s), 1261 (m), 1212 (w), 1172 (w), 1128 (m), 1102 (m), 1083 (m), 1067 (m), 1029 (m), 997 (w), 986 (w), 975 (w), 875 (w), 801 (m), 756 (m), 726 (m), 701 (m), 627 (w), 612 (w), 507 (w), 488 (w), 444 (w), 428 (w), 410 (m) cm^{-1} . ¹H NMR (C₅D₅N, 25°C): 7.62 (2H, $w_{1/2} = 151$ Hz), 7.30 (3H, $w_{1/2} = 134$ Hz). These resonances are probably due to rapidly exchanging free and coordinated pyridine ligands. The compound has an absorption maximum in pyridine ($\lambda_{\text{max}} = 350$ nm) and an intense shoulder that tails out beyond 500 nm.

(BIPY)(THF)₂Eu(S-2-C₅H₄N)₂ (2). Compound **1** (0.90 g, 1.3 mmol) and bipyridine (0.61 g, 3.7 mmol) were dissolved in THF (30 mL). After 1 h the dark brown solution was concentrated (10 mL), heated to dissolve the precipitate, and again cooled (-20°C) to give **2** (0.70 g, 77%). Complex **2** does not appear to melt below 300°C but turns orange above 240°C . The THF ligands are lost rapidly at room temperature when the compound is isolated from the mother liquor. Anal. Calcd for C₂₆H₁₆N₆EuS₂: C, 45.5; H, 3.06; N, 10.6. Found: C, 45.5; H, 3.01; N, 10.8. λ_{max} : 355 nm (THF). The compound is sparingly soluble in THF, and redissolving crystalline **2** in THF results in displacement of the BIPY ligand and the precipitation of an insoluble light yellow compound. In an attempt to unambiguously determine the energy of the Eu-to-BIPY charge transfer absorption, **2** was dissolved in the presence of a large excess of BIPY, but no distinct new peaks were observed. Addition of BIPY (10 mg) to a solution of **2** (2 mg) in THF (1 mL) resulted in a shift in the value of λ_{max} to 365 nm and also shifted the position of the absorption tail to lower energy. λ_{max} : 351 nm (pyridine). IR: 2923 (s), 2855 (s), 1578 (w), 1536 (w), 1460 (s), 1406 (w), 1377 (s), 1310 (w), 1260 (w), 1128 (w), 1098 (w), 1038 (w), 803 (w), 761 (w), 724 (w) cm^{-1} . ¹H NMR (C₅D₅N, 25°C): 7.63 ($w_{1/2} = 143$ Hz), 7.26 ($w_{1/2} = 130$ Hz), 3.81 ($w_{1/2} = 80.6$ Hz), 1.73 ($w_{1/2} = 44.5$ Hz).

[PEt₄][Eu(S-2-NC₅H₄)₄] (3). 2-Mercaptopyridine (0.90 g, 8.1 mmol) was dissolved in THF (50 mL) and NaHBEt₃ (7.2 mL of a 1.0 M solution in THF, 7.2 mmol) was added via syringe. This solution was

- (4) (a) Pomrenke, G. S.; Klein, P. B.; Langer, D. W. *Rare Earth Doped Semiconductors* (MRS Symposium V.301); Materials Research Society: Pittsburgh, PA, 1993. (b) Singer, K. E.; Rutter, P.; Praker, A. R.; Wright, A. C. *Appl. Phys. Lett.* **1994**, *64*, 707–9. (c) Swiatek, K.; Godlewski, M.; Niinistö, L.; Leskela, M. *J. Appl. Phys.* **1993**, *74*, 3442–6. (d) Taniguchi, M.; Takahei, K. *J. Appl. Phys.* **1993**, *73*, 943–7. (e) Jourdan, N.; Yamaguchi, H.; Harikoshi, Y. *Jpn. J. Appl. Phys.* **1993**, *32* (2), 1784–7. (f) Kalbousi, A.; Moneger, S.; Marrakchi, G.; Guillot, G.; Lambert, B.; Guivarc'h, A. *J. Appl. Phys.* **1994**, *75*, 4171–5. (g) Takahei, K.; Taguchi, A.; Harikoshi, Y.; Nakata, J. *J. Appl. Phys.* **1994**, *76*, 4332–9. (h) Lozykowski, H. J.; Alshawa, A. K.; Brown, I. *J. Appl. Phys.* **1994**, *76*, 4836–46. (i) Kimura, T.; Isshiki, H.; Ishida, H.; Yugo, S.; Saito, R.; Ikoma, T. *J. Appl. Phys.* **1994**, *76*, 3714–9. (j) Karpinska, K.; Godlewski, M.; Leskelä, L.; Niinistö, L. *J. Alloys and Compounds* **1995**, *225*, 544–6. (k) Charreire, Y.; Marbeuf, A.; Tourillon, G.; Leskela, M.; Niinistö, L.; Nykanen, E.; Soininen, P.; Tolonen, O. *J. Electrochem. Soc.* **1992**, *139*, 619–21. (l) Charreire, Y.; Svoronos, D. R.; Ascone, I.; Tolonen, O.; Niinistö, L.; Leskela, M. *J. Electrochem. Soc.* **1993**, *140*, 2015–9.
- (5) (a) Kanamori, T.; Terunuma, Y.; Takahashi, S.; Miyashita, T. *J. Lightwave Tech.* **1984**, *LT2*, 607. (b) Kumta, P. N.; Rishbud, S. H. *Ceramic Bull.* **1990**, *69*, 1977. (c) Nishii, J.; Morimoto, S.; Yokota, R.; Yamagishi, T. *J. Non-Cryst. Solids* **1987**, *95/96*, 641–6. (d) Savage, J. A. In *Infrared Optical Materials and Their Antireflection Coatings*; Adam Hilger Ltd: Bristol, U.K., 1985; pp 79–94. (e) Nishii, J.; Morimoto, S.; Inagawa, I.; Iizuka, R.; Yamashita, T.; Yokota, R.; Yamagishi, T. *J. Non-Cryst. Solids* **1992**, *140*, 199–208. (f) Sanghara, J. S.; Busse, L. E.; Aggarwall, I. D. *J. Appl. Phys.* **1994**, *75*, 4885–91. (g) Katsugama, T.; Matsumura, H. *J. Appl. Phys.* **1994**, *75*, 2743–8.
- (6) (a) Brown, D.; Holah, D. G.; Rickard, C. E. *J. Chem. Soc. A* **1970**, 786–90. (b) Ciaopolini, M.; Nardi, N.; Colamarino, P.; Orioli, P. *J. Chem. Soc., Dalton Trans.* **1977**, 379. (c) Pinkerton, A. A.; Meseri, Y.; Rieder, C. *J. Chem. Soc., Dalton Trans.* **1978**, 85. (d) Pinkerton, A. A.; Schwartzenback, D. *J. Chem. Soc., Dalton Trans.* **1976**, 2466.

- (7) (a) Umakoshi, K.; Kinoshita, I.; Ichimura, A.; Ooi, S. *Inorg. Chem.* **1987**, *26*, 3551–6. (b) Baghlaif, A. O.; Ishaq, M.; Rashed, A. K. A. *Polyhedron* **1987**, *6*, 837–9. (c) Brandenberg, K. L.; Heeg, M. J.; Abrahamson, H. B. *Inorg. Chem.* **1987**, *26*, 1064–9. (d) Umakoshi, K.; Kinoshita, I.; Ooi, S. *Inorg. Chim. Acta* **1987**, *127*, L41–2. (e) Rosenfield, S. G.; Berends, H. P.; Gelmini, L.; Stephan, D. W.; Mascharak, P. K. *Inorg. Chem.* **1987**, *26*, 2792–7. (f) Deeming, A. J.; Hardcastle, K. I.; Meah, M. N.; Bates, P. A.; Dawes, H. M.; Hursthouse, M. B. *J. Chem. Soc., Dalton Trans.* **1988**, 227–33. (g) Deeming, A. J.; Meah, M. N.; Bates, P.; Hursthouse, M. B. *J. Chem. Soc., Dalton Trans.* **1988**, 2193–9. (h) Kumar, R.; de Mel, V.; Oliver, J. P. *Organometallics* **1989**, *8*, 2488–90. (i) Wang, S.; Fackler, J. P. *Inorg. Chem.* **1989**, *28*, 2615. (j) Ainscough, E. W.; Baker, E. N.; Bingham, A. G.; Brodie, A. W.; Smith, C. A. *J. Chem. Soc., Dalton Trans.* **1989**, 2167–71. (k) Ciriano, M. A.; Viguri, F.; Perez-Torrente, J. J.; Lahoz, F. J.; Oro, L. A.; Tiripicchio, A.; Camellini, M. *J. Chem. Soc., Dalton Trans.* **1989**, 25–32. (l) Umakoshi, K.; Kinoshita, I.; Fukui, Y.; Matsumoto, K.; Ooi, S.; Nakai, H.; Shiro, M. *J. Chem. Soc., Dalton Trans.* **1989**, 815–9. (m) Kita, M.; Yamanari, K.; Shimura, Y. *Bull. Chem. Soc. Jpn.* **1989**, *62*, 3081–8. (n) Castano, M. V.; Macias, A.; Castineiras, A.; Gonzalez, A. S.; Martinez, E. G.; Casas, J. S.; Sordo, J.; Hiller, W.; Castellano, E. E. *J. Chem. Soc., Dalton Trans.* **1990**, 1001–5. (o) Deeming, A. J.; Meah, M. N.; Randel, N. P.; Hardcastle, K. I. *J. Chem. Soc., Dalton Trans.* **1990**, 2211–6. (p) Deeming, A. J.; Karim, M.; Powell, N. I. *J. Chem. Soc., Dalton Trans.* **1990**, 2321–4. (q) Castro, R.; Duran, M. L.; Garcia-Vasquez, J. A.; Romero, J.; Sousa, A.; Castineiras, A.; Hiller, W.; Strahle, J. *J. Chem. Soc., Dalton Trans.* **1990**, 531–4. (r) Yamamoto, J. H.; Yoshida, W.; Jensen, C. M. *Inorg. Chem.* **1991**, *30*, 1353–7.

stirred for 30 min, and the solvent was removed under vacuum to leave a white solid. Hg (0.1 g, 0.5 mmol), Eu (1.1 g, 7.2 mmol), 2,2'-dithiodipyridine (10.8 g, 2.4 mmol), Et₄PCl (1.3 g, 7.2 mmol), and CH₃CN (50 mL) were added to the white solid, and the solution was refluxed for 18 h. The bright orange solution was filtered and concentrated (20 mL). The solution was refluxed to redissolve precipitated material and then cooled (-20 °C) to give crystals of **3** (3.5 g, 67%, mp 260–265 °C) that were collected by filtration. Anal. Calcd for C₂₈H₃₆N₄EuPS₄: C, 45.5; H, 4.91; N, 7.57. Found: C, 45.5; H, 4.96; N, 7.65. IR: 2972 (s), 1856 (w), 1724 (w), 1580 (s), 1537 (m), 1460 (s), 1447 (s), 1407 (s), 1379 (s), 1261 (m), 1227 (w), 1178 (w), 1151 (w), 1129 (s), 1086 (m), 997 (m), 973 (w), 759 (s), 727 (s), 635 (m), 487 (m), 448 (m), 406 (m) cm⁻¹. ¹H NMR (C₅D₅N, 20 °C): 6.88 (4H, t), 6.54 (4H, m), 3.43 (8H, m), 2.75 (4H, d), 1.77 (12H, m), 1.52 (4H, m). ¹³C NMR (C₅D₅N, 20 °C): 148.9, 135.3, 107.9, 103.0, 69.7, 11.57 (d, *J*_{C-P} = 45 Hz), 5.73. λ_{max}: 358 nm (ε = 340 M⁻¹ cm⁻¹) (THF), 420 (ε = 213 M⁻¹ cm⁻¹). Only a single set of ¹H NMR resonances were detected even when the temperature of the sample was lowered to -50 °C. A plot of ¹H NMR chemical shift vs 1/*T* showed only ideal Curie–Weiss behavior for all four proton resonances. Compound **3** does not sublime intact.

Thermolysis. Compound **3** (0.60 g, 0.81 mmol) was placed in a Pyrex tube under vacuum for 1 h. The tube was then sealed and the sample temperature was raised over 24 h from 50 to 500 °C with one end of the tube kept outside the oven at room temperature. Between 250 and 300 °C a yellow liquid and colorless crystals condensed in the cool end of the tube. As the temperature was raised above 300 °C an amber liquid began to condense in the cold zone. At 400 °C a substantial quantity of amber liquid had condensed, and no further condensation was observed. The cold end of the tube was placed in liquid nitrogen, and the furnace temperature was raised to 500 °C. After 24 h both the volatile and the condensed solid materials were isolated and analyzed. ¹H NMR analysis of the volatile products revealed the absence of dipyrindinyldisulfide and a complex mixture of aromatic and phosphorus-containing products. GCMS gave M⁺ molecular ions (relative abundances in []) for PySSPy [5], PySPy [42], SPEt₃ [10], and PySEt [14]. X-ray powder diffraction indicated that the only crystalline phase of the final solid state product was EuS (0.15 g, 100%).

X-ray Structure Determination of 1, 2, and 3. Data for **1–3** were collected on a CAD4 diffractometer with graphite-monochromatized Mo Kα radiation, λ = 0.710 73 Å at low temperatures (153 K). The crystals were isolated and immersed (within seconds) in dry, degassed Paratone oil and examined under a polarizing microscope. All samples were mounted on a glass fiber within minutes of isolation from the mother liquor and cooled rapidly, in order to minimize problems related to neutral ligand dissociation. In all structures, three check reflections were measured every 3 h and showed no significant intensity variation. The data were corrected for Lorentz effects and polarization. The absorption corrections for **2** and **3** were based on a Gaussian grid method (SHELX76).⁸ The structures were solved by Patterson and direct methods (SHELXS86).⁹ All non-hydrogen atoms were refined (SHELXL93)¹⁰ on the basis of *F*_{obs}². All hydrogen atom coordinates were calculated with idealized geometries (SHELXL93). Scattering factors (*f*₀, *f*, *f'*) are as described in SHELXL93. Crystallographic data and final *R* indices are given in Table 1. Complete crystallographic details are given in the supporting information.

Results and Discussion

Synthesis and Structural Characterization. Europium forms stable divalent and trivalent complexes with the pyridine-2-thiolate ligand. The divalent europium pyridinethiolate (pyridine)₄Eu(S-2-NC₅H₄)₂ (**1**) was best prepared from the transmetalation reaction of Eu with Hg(S-2-NC₅H₄)₂ in pyridine (reaction 1). There is no apparent reaction in THF. Once isolated compound **1** rapidly desolvates just as found for the

Table 1. Crystal Data and Structure Refinement for (py)₄Eu(S-2-NC₅H₄)₂ (**1**), (BIPY)(THF)₂Eu(S-2-NC₅H₄)₂ (**2**), and [PEt₄][Eu(S-2-NC₅H₄)₄] (**3**)^a

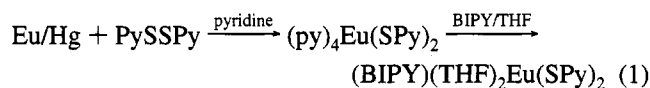
	1	2	3
empirical formula	C ₃₀ H ₂₈ EuN ₆ S ₂	C ₂₈ H ₃₂ EuN ₄ O ₂ S ₂	C ₅₆ H ₇₂ Eu ₂ N ₈ P ₂ S ₈
formula weight	688.66	672.66	1479.56
space group	<i>Pna</i> 2/1	Cc	<i>P2</i> ₁ / <i>n</i>
<i>a</i> (Å)	19.006(2)	9.851(2)	15.043(3)
<i>b</i> (Å)	9.724(5)	16.817(3)	16.036(6)
<i>c</i> (Å)	15.592(5)	17.271(2)	26.444(5)
α (deg)	90	90	90
β (deg)	90	92.67(2)	90.54(2)
γ (deg)	90	90	90
volume (Å ³)	2882(2)	2858.1(8)	6379(3)
<i>Z</i>	4	4	4
density (calcd) (mg/m ³)	1.587	1.563	1.541
temperature (K)	153	153	153
λ (Å)	0.71073	0.71073	0.71073
absorption coeff (mm ⁻¹)	2.352	2.372	2.303
obs reflections	1748	2492	6626
final <i>R</i> (<i>F</i>) [<i>I</i> > 2σ]	0.030	0.032	0.032
<i>R</i> _w (<i>F</i> ²) indices [<i>I</i> > 2σ]	0.071	0.068	0.075

^a Definitions: *R*(*F*_o) = Σ||*F*_o| - |*F*_c||/Σ|*F*_o|; *R*_w(*F*_o²) = {Σ[*w*(*F*_o² - *F*_c²)²]/Σ[*w*(*F*_o²)²]}^{1/2}. Additional crystallographic details are given in the supporting information.

Table 2. Significant Bond Lengths (Å) and Angles (deg) for **1**

Eu–N(1)	2.691(9)	Eu–N(2)	2.694(8)
Eu–N(3)	2.722(9)	Eu–N(6)	2.728(9)
Eu–N(4)	2.738(10)	Eu–N(5)	2.818(10)
Eu–S(1)	3.025(3)	Eu–S(2)	3.066(4)
S(1)–C(1)	1.726(11)	S(2)–C(6)	1.719(13)
N(1)–Eu–N(2)	89.5(3)	N(1)–Eu–N(3)	76.3(3)
N(2)–Eu–N(3)	92.0(3)	N(1)–Eu–N(6)	132.9(3)
N(2)–Eu–N(6)	128.8(3)	N(3)–Eu–N(6)	76.2(3)
N(1)–Eu–N(4)	119.0(3)	N(2)–Eu–N(4)	115.1(3)
N(3)–Eu–N(4)	147.6(3)	N(6)–Eu–N(4)	73.0(3)
N(1)–Eu–N(5)	73.1(3)	N(2)–Eu–N(5)	69.8(3)
N(3)–Eu–N(5)	144.2(3)	N(6)–Eu–N(5)	139.3(3)
N(4)–Eu–N(5)	66.4(3)	N(1)–Eu–S(1)	54.8(2)
N(2)–Eu–S(1)	144.0(2)	N(3)–Eu–S(1)	84.4(2)
N(6)–Eu–S(1)	85.1(2)	N(4)–Eu–S(1)	83.3(2)
N(5)–Eu–S(1)	92.7(2)	N(1)–Eu–S(2)	138.9(2)
N(2)–Eu–S(2)	53.9(2)	N(3)–Eu–S(2)	86.1(2)
N(6)–Eu–S(2)	75.4(2)	N(4)–Eu–S(2)	95.6(2)
N(5)–Eu–S(2)	105.2(2)	S(1)–Eu–S(2)	159.92(9)
C(1)–S(1)–Eu	82.9(4)	C(6)–S(2)–Eu	83.6(6)

majority of divalent lanthanide chalcogenolate complexes containing neutral monodentate ligands.



The structure of **1** was determined by low-temperature single-crystal X-ray diffraction. Table 1 gives a listing of crystallographic details, Table 2 gives a listing of significant bond lengths and angles, and Figure 1 gives an ORTEP diagram for **1**. From the structure it is clear from the Eu–S and Eu–N bond lengths that the Eu ion is divalent. The Eu–S distances in **1** (3.025(3) and 3.066(4) Å) are considerably longer than the terminal Eu–S distance of 2.898(4) Å in the divalent thiolate [Eu(S-2,4,6-tri-*i*-pr-C₆H₂)₂THF₃]₂ but statistically equivalent to the bridging Eu–S distances (3.030(3) and 3.001(3) Å)^{3k} within the same structure. The Eu–S distances in **1** are also statistically equivalent to the bridging Eu–S distances in the heterometallic phenylthiolates¹¹ [(py)₃EuHg(SPh)₄]₂ (3.03(1) Å), [(py)₃EuCd-

(8) Sheldrick, G. M. *SHELX76, Program for Crystal Structure Determination*; University of Cambridge: England, 1976.

(9) Sheldrick, G. M. *SHELXS86, Program for the Solution of Crystal Structures*; University of Göttingen: Germany, 1986.

(10) Sheldrick, G. M. *SHELXL93, Program for Crystal Structure Refinement*; University of Göttingen: Germany, 1993.

(11) Brewer, M.; Lee, J.; Brennan, J. *Inorg. Chem.* **1995**, *34*, 5919–24.

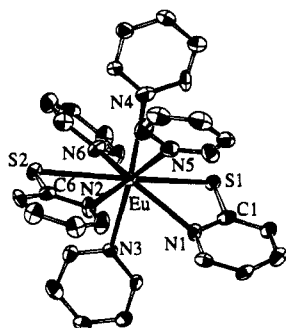


Figure 1. Molecular structure of $(\text{py})_4\text{Eu}(\text{S}-2\text{-NC}_5\text{H}_4)_2$ (**1**).

Table 3. Significant Bond Lengths (Å) and Angles (deg) for **2**

Eu—O(1)	2.555(10)	Eu—O(2)	2.615(7)
Eu—N(3)	2.678(8)	Eu—N(2)	2.716(14)
Eu—N(4)	2.712(14)	Eu—N(1)	2.754(13)
Eu—S(2)	3.002(2)	Eu—S(1)	3.011(3)
S(1)—C(1)	1.741(12)	S(2)—C(6)	1.73(2)
O(1)—Eu—O(2)	150.3(3)	O(1)—Eu—N(3)	86.1(3)
O(2)—Eu—N(3)	83.0(3)	O(1)—Eu—N(2)	130.2(4)
O(2)—Eu—N(2)	75.6(3)	N(3)—Eu—N(2)	82.5(3)
O(1)—Eu—N(4)	75.3(4)	O(2)—Eu—N(4)	75.3(3)
N(3)—Eu—N(4)	60.1(3)	N(2)—Eu—N(4)	134.7(2)
O(1)—Eu—N(1)	120.1(2)	O(2)—Eu—N(1)	77.5(3)
N(3)—Eu—N(1)	152.4(3)	N(2)—Eu—N(1)	73.9(4)
N(4)—Eu—N(1)	131.0(4)	O(1)—Eu—S(2)	76.6(2)
O(2)—Eu—S(2)	130.4(2)	N(3)—Eu—S(2)	88.5(2)
N(2)—Eu—S(2)	54.8(3)	N(4)—Eu—S(2)	138.8(3)
N(1)—Eu—S(2)	89.4(3)	O(1)—Eu—S(1)	83.1(2)
O(2)—Eu—S(1)	90.6(2)	N(3)—Eu—S(1)	146.0(2)
N(2)—Eu—S(1)	128.3(3)	N(4)—Eu—S(1)	85.9(3)
N(1)—Eu—S(1)	54.4(3)	S(2)—Eu—S(1)	119.79(7)
C(1)—S(1)—Eu	82.3(3)	C(6)—S(2)—Eu	81.4(5)

(SPh)₄]₂ (3.02(1) Å), and [(THF)₃EuZn(SPh)₄]₂ (2.99(1) Å). A comparison of the C—S bond lengths (avg 1.72 Å) in **1** with the short C—S double bond of the protonated ligand S-2-C₅H₄-NH (1.69 Å)^{12a} and the ideal value (1.81 Å) for a C—S single bond^{12b} indicates that the thioketone/metal amido resonance structure does contribute to overall complex stability. The C—S bonds in **1** are within 0.02 Å of the related bond lengths in the majority of pyridinethiolate metal complexes.⁷

In an attempt to form a complex that was stable with respect to ligand dissociation at room temperature, $(\text{py})_4\text{Eu}(\text{S}-2\text{-NC}_5\text{H}_4)_2$ was reacted with an excess of 2,2'-bipyridine (BIPY) in THF. Crystallization of the dark brown reaction product from THF gave an intensely colored compound that, surprisingly, appeared to be even less stable than the pyridine complex **1**, with isolated crystals becoming opaque within minutes of isolation. Low-temperature single-crystal X-ray diffraction revealed the origins of the thermal instability by showing that BIPY does not completely displace THF from the metal coordination sphere of the isolated compound and instead $(\text{BIPY})(\text{THF})_2\text{Eu}(\text{S}-2\text{-NC}_5\text{H}_4)_2$ (**2**) is isolated in 77% yield. Table 1 gives a listing of crystallographic details, Table 3 gives a listing of significant bond lengths and angles, and Figure 2 gives an ORTEP diagram for **2**. Again, it is clear from the Eu—S and Eu—N bond lengths that the Eu ion is divalent in **2**. The Eu—S bond lengths (3.002(2) and 3.011(3) Å) and average Eu—N (2.72(2) Å) distances in **2** are virtually identical to the bond geometries in **1**.

The THF ligands in **2** are not detectable by elemental analysis, but resonances attributable to THF ligands can be observed in the ¹H NMR spectrum, which is unfortunately too broad ($w_{1/2}$

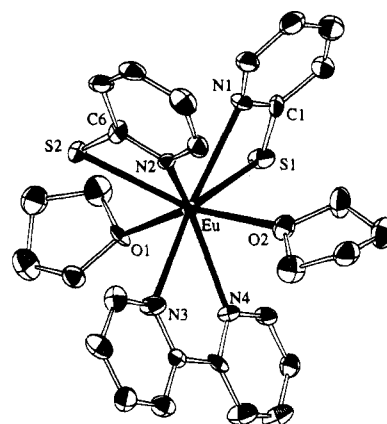
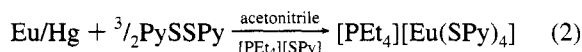


Figure 2. Molecular structure of $(\text{BIPY})(\text{THF})_2\text{Eu}(\text{S}-2\text{-NC}_5\text{H}_4)_2$ (**2**).

ca. 45 Hz for the THF ligands and ca. 150 Hz for the aromatic resonances) for accurate integration. The rapidity with which **2** loses neutral donor ligands relative to **1** can easily be attributed to the weaker donor strength of the THF ligands, which have shown a tendency to dissociate rapidly even from trivalent lanthanide chalcogenolate complexes. The BIPY ligands are also readily displaced from the metal coordination sphere. Complex **2** is initially soluble in THF but subsequently reacts with the solvent to form a light yellow, BIPY free precipitate. This precipitation can be inhibited by the addition of excess BIPY to the solution. Further, in pyridine solution the identical optical spectra of **1** and **2** suggest complete displacement of the BIPY and THF ligands by pyridine.

A thioketone/metal amido resonance structure increases the ability of the pyridinethiolate ligand to stabilize higher oxidation states of ionic metals, relative to arenethiolate ligands. This is most important in Eu chalcogenolate chemistry which has to date been limited to the divalent oxidation state. We initially approached the synthesis of europium(III) 2-pyridinethiolate complexes from the reaction of EuCl_3 with 3 equiv of NaS-2-NC₅H₄, and there were two important observations in this work. First, it became clear that, in contrast to metathetical syntheses of $\text{Eu}(\text{SePh})_2$ ^{3e} and $\text{Eu}(\text{TePh})_2$ ^{3f} in which diphenyl dichalcogenide formation was observed, with the pyridinethiolate ligand there was no reductive elimination of disulfide, and thus it appeared that pyridinethiolate anions were capable of stabilizing Eu(III). Second, what we perceived as $\text{Eu}(\text{S}-2\text{-NC}_5\text{H}_4)_3$ was insoluble in all conventional donor solvents. The solubility of Eu-containing material could be enhanced by using a 4:1 NaSPy: EuCl_3 ratio, but the resulting crystalline heterometallic (Na/Eu) pyridinethiolate compounds usually melted below room temperature and were impossible to characterize unambiguously. With this information it was clear that a 4:1 S-2-NC₅H₄:Eu ratio with a cation that did not contain labile monodentate neutral donor ligands offered the most likely chance of isolating a characterizable Eu(III) complex.

The most efficient synthesis of a Eu(III) pyridinethiolate complex was found to be a simple reduction of the disulfide with a Eu/Hg amalgam. The reaction of $3/2\text{PySSPy}$ with Eu/Hg in the presence of $[\text{PEt}_4][\text{SPy}]$ gave $[\text{PEt}_4][\text{Eu}(\text{S}-2\text{-NC}_5\text{H}_4)_4]$ (**3**) in 67% yield (reaction 2). Molecular **3** was characterized



by low temperature single-crystal X-ray diffraction. Table 1 gives a listing of crystallographic details for **3**, and Table 4 gives a list of significant bond geometries for **3**. The unit cell contains three inequivalent eight-coordinate Eu(III) ions with differing arrangements of chelating pyridinethiolate ligands. Figure 3

(12) (a) Ohms, U.; Guth, H.; Kutoglu, A.; Scheringer, C. *Acta Crystallogr. B* **1982**, *38*, 831. (b) Curry, J. D.; Jandecsek, R. J. *J. Chem. Soc., Dalton Trans.* **1972**, 1120.

Table 4. Significant Bond Lengths (Å) and Angles (deg) for the Anions in **3**

Eu(1)–N(2)	2.499(4)	Eu(1)–N(4)	2.530(4)
Eu(1)–N(1)	2.532(4)	Eu(1)–N(3)	2.535(4)
Eu(1)–S(1)	2.838(2)	Eu(1)–S(3)	2.846(2)
Eu(1)–S(4)	2.858(2)	Eu(1)–S(2)	2.885(2)
Eu(1)–C(11)	3.124(5)	Eu(1)–C(1)	3.130(5)
S(1)–C(1)	1.743(5)	S(3)–C(11)	1.729(5)
S(2)–C(6)	1.740(5)	S(4)–C(16)	1.740(6)
Eu(2)–N(5')	2.522(4)	Eu(2)–N(5)	2.522(4)
Eu(2)–N(6')	2.527(4)	Eu(2)–N(6)	2.527(4)
Eu(2)–S(5)	2.853(1)	Eu(2)–S(5')	2.853(1)
Eu(2)–S(6)	2.873(2)	Eu(2)–S(6')	2.873(2)
S(5)–C(21)	1.753(5)	S(6)–C(26)	1.736(5)
Eu(3)–N(7)	2.502(4)	Eu(3)–N(7)''	2.502(4)
Eu(3)–N(8)	2.507(4)	Eu(3)–N(8)''	2.507(4)
Eu(3)–S(8)''	2.843(2)	Eu(3)–S(8)	2.843(2)
Eu(3)–S(7)''	2.910(2)	Eu(3)–S(7)	2.910(2)
S(7)–C(31)	1.742(5)	S(8)–C(36)	1.742(5)
N(2)–Eu(1)–N(4)	76.72(13)	N(2)–Eu(1)–N(1)	159.03(14)
N(4)–Eu(1)–N(1)	111.30(14)	N(2)–Eu(1)–N(3)	83.29(13)
N(4)–Eu(1)–N(3)	132.93(14)	N(1)–Eu(1)–N(3)	77.24(13)
N(2)–Eu(1)–S(1)	143.01(10)	N(4)–Eu(1)–S(1)	84.54(10)
N(1)–Eu(1)–S(1)	57.94(10)	N(3)–Eu(1)–S(1)	131.26(10)
N(2)–Eu(1)–S(3)	90.20(10)	N(4)–Eu(1)–S(3)	160.26(11)
N(1)–Eu(1)–S(3)	86.12(10)	N(3)–Eu(1)–S(3)	58.11(10)
S(1)–Eu(1)–S(3)	97.90(5)	N(2)–Eu(1)–S(4)	86.28(11)
N(4)–Eu(1)–S(4)	58.16(11)	N(1)–Eu(1)–S(4)	82.34(10)
N(3)–Eu(1)–S(4)	78.61(10)	S(1)–Eu(1)–S(4)	110.46(5)
S(3)–Eu(1)–S(4)	136.68(5)	N(2)–Eu(1)–S(2)	58.22(10)
N(4)–Eu(1)–S(2)	77.52(11)	N(1)–Eu(1)–S(2)	141.26(10)
N(3)–Eu(1)–S(2)	125.49(10)	S(1)–Eu(1)–S(2)	86.89(4)
S(3)–Eu(1)–S(2)	83.04(5)	S(4)–Eu(1)–S(2)	129.05(5)
C(1)–S(1)–Eu(1)	82.5(2)	C(6)–S(2)–Eu(1)	81.3(2)
C(11)–S(3)–Eu(1)	82.3(2)	C(16)–S(4)–Eu(1)	82.3(2)
N(5)'–Eu(2)–N(5)	76.8(2)	N(5)'–Eu(2)–N(6)'	121.84(13)
N(5)–Eu(2)–N(6)'	130.99(13)	N(5)'–Eu(2)–N(6)	130.99(13)
N(5)–Eu(2)–N(6)	121.84(13)	N(6)'–Eu(2)–N(6)	82.0(2)
N(5)'–Eu(2)–S(5)	86.40(10)	N(5)–Eu(2)–S(5)	58.28(9)
N(6)'–Eu(2)–S(5)	76.85(10)	N(6)–Eu(2)–S(5)	142.61(10)
N(5)'–Eu(2)–S(5')	58.28(9)	N(5)–Eu(2)–S(5')	86.40(10)
N(6)'–Eu(2)–S(5')	142.60(10)	N(6)–Eu(2)–S(5')	76.84(10)
S(5)–Eu(2)–S(5')	135.89(6)	N(5)'–Eu(2)–S(6)	149.64(10)
N(5)–Eu(2)–S(6)	75.80(10)	N(6)'–Eu(2)–S(6)	86.44(10)
N(6)–Eu(2)–S(6)	57.81(10)	S(5)–Eu(2)–S(6)	90.17(4)
S(5)'–Eu(2)–S(6)	107.03(4)	N(5)'–Eu(2)–S(6)'	75.80(10)
N(5)–Eu(2)–S(6)'	149.64(10)	N(6)'–Eu(2)–S(6)'	57.81(10)
N(6)–Eu(2)–S(6)'	86.44(10)	S(5)–Eu(2)–S(6)'	107.03(4)
S(5)'–Eu(2)–S(6)'	90.17(4)	S(6)–Eu(2)–S(6)'	133.60(6)
C(21)–S(5)–Eu(2)	81.5(2)	C(26)–S(6)–Eu(2)	81.8(2)
N(7)–Eu(3)–N(7)''	77.5(2)	N(7)–Eu(3)–N(8)	99.98(14)
N(7)''–Eu(3)–N(8)	171.21(13)	N(7)–Eu(3)–N(8)''	171.21(13)
N(7)''–Eu(3)–N(8)''	99.98(14)	N(8)–Eu(3)–N(8)''	83.7(2)
N(7)–Eu(3)–S(8)''	129.66(10)	N(7)''–Eu(3)–S(8)''	86.96(11)
N(8)–Eu(3)–S(8)''	88.32(10)	N(8)''–Eu(3)–S(8)''	58.03(10)
N(7)–Eu(3)–S(8)	86.96(11)	N(7)''–Eu(3)–S(8)	129.66(10)
N(8)–Eu(3)–S(8)	58.03(10)	N(8)''–Eu(3)–S(8)	88.32(10)
S(8)''–Eu(3)–S(8)	135.93(6)	N(7)–Eu(3)–S(7)''	84.49(10)
N(7)''–Eu(3)–S(7)''	56.98(10)	N(8)–Eu(3)–S(7)''	131.51(10)
N(8)''–Eu(3)–S(7)''	87.09(10)	S(8)''–Eu(3)–S(7)''	125.45(4)
S(8)–Eu(3)–S(7)''	74.23(4)	N(7)–Eu(3)–S(7)	56.97(10)
N(7)''–Eu(3)–S(7)	84.50(10)	N(8)–Eu(3)–S(7)	87.09(10)
N(8)''–Eu(3)–S(7)	131.51(10)	S(8)''–Eu(3)–S(7)	74.24(4)
S(8)–Eu(3)–S(7)	125.45(4)	S(7)''–Eu(3)–S(7)	131.48(6)
C(31)–S(7)–Eu(3)	81.4(2)	C(36)–S(8)–Eu(3)	82.8(2)

shows ORTEP diagrams for the three anions in the structure of **3**. Two isomers (Eu2 and Eu3, Figure 3b and c, respectively) contain symmetry related pyridinethiolate ligands that differ in the relative proximity of the donor types. For Eu2, the S–Eu–S angles are S(5)–Eu(2)–S(5') (135.89(6)°), S(5)–Eu(2)–S(6) (90.17(4)°), S(5)'–Eu(2)–S(6) (107.03(4)°), S(5)–Eu(2)–S(6)' (107.03(4)°), S(5)'–Eu(2)–S(6)' (90.17(4)°), and S(6)–Eu(2)–S(6)' (133.60(6)°). For Eu3, the S–Eu–S angles are S(8)''–

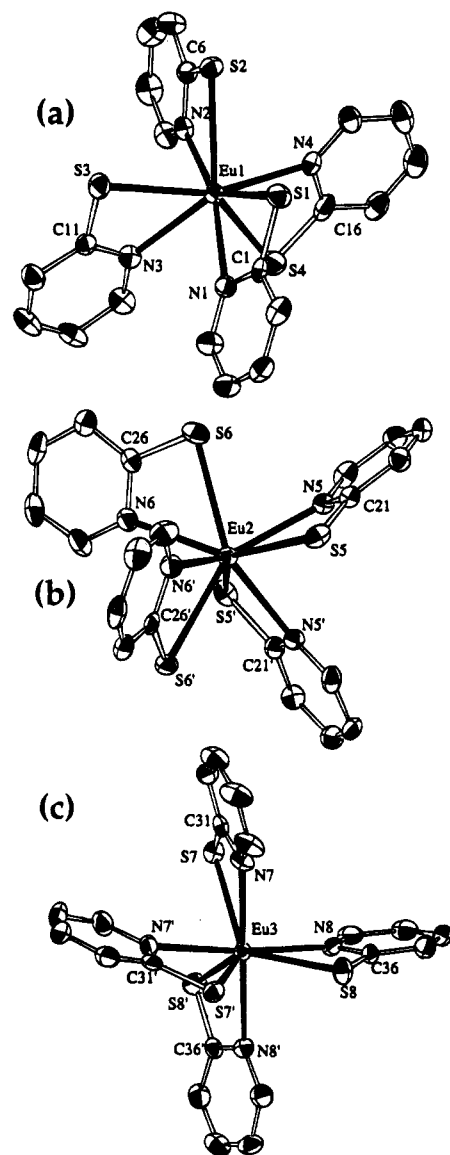


Figure 3. Molecular structure of the three different anions in the unit cell of $[\text{PEu}_4][\text{Eu}(\text{S}-2\text{-NC}_5\text{H}_4)_4]$ (**3**). Each isomer has a different relative orientation of the pyridinechalcogenolate ligands, and all have statistically equivalent europium–ligand bond lengths.

Eu(3)–S(8) (135.93(6)°), S(8)''–Eu(3)–S(7)'' (125.45(4)°), S(8)–Eu(3)–S(7)'' (74.23(4)°), S(8)''–Eu(3)–S(7) (74.24(4)°), S(8)–Eu(3)–S(7) (125.45(4)°), and S(7)''–Eu(3)–S(7) (131.48(6)°). The remaining Eu (Eu1, Figure 1a) differs in having no symmetry-related ligands, and there are three adjacent sulfur atoms (S1, S2, S3) and one sulfur (S4) at a further distance from the three. The S–Eu–S angles are S(1)–Eu(1)–S(3) (97.90(5)°), S(1)–Eu(1)–S(4) (110.46(5)°), S(3)–Eu(1)–S(4) (136.68(5)°), S(1)–Eu(1)–S(2) (86.89(4)°), S(3)–Eu(1)–S(2) (83.04(5)°), and S(4)–Eu(1)–S(2) (129.05(5)°). The cocrystallization of three structural forms of a single molecule within a single unit cell suggests that the potential energy surface defining the stability of the coordination geometry of this europium pyridinethiolate structure is relatively shallow (as are potential energy surfaces defining eight-coordinate geometries in general). This interpretation is supported by a variable-temperature NMR experiment that revealed the presence of only a single set of pyridinethiolate resonances at a temperature as low as -50°C . The resonances all shift linearly as a function of $1/T$, and so either there is only one solution structure with equivalent ligand environments or the exchange of inequivalent sites is rapid on an NMR time scale.

The average bond length data (Eu–S = 2.87(2) Å and Eu–N = 2.52(1) Å) are indicative of a trivalent Eu ion. The average Eu–S distance and average Eu–N distance in **3** are shorter, by 0.15 and 0.21 Å, respectively, than the related distances in **1** or **2**. This decrease in metal–ligand bond lengths upon increase in metal oxidation state is expected in ionic chemistry: ionic radii tables compiled by Shannon¹³ predict a difference of 0.18 Å between eight-coordinate compounds of Eu(II) and Eu(III).

The nonaqueous chemistry of Eu(III) is limited by the relative stability of the divalent oxidation state, and this is particularly noticeable when a discussion excludes halides or nonoxygen-based ligands. Known compounds such as Eu(N(SiMe₃)₂)₃,¹⁴ the dithiocarbamates Eu(S₂CNR₂)₃,^{6a,b} and the dithiophosphates Eu(S₂PR₂)₃,^{6c,d} represent the best characterized examples of this class of compounds, which was expanded just recently to include the first organometallic derivative of Eu(III), (C₅Me₅)₂Eu(OCMe₃).¹⁵ The resonance-stabilized sulfur derivatives and the electron-withdrawing silylamides both supported the presumption that a resonance-stabilized pyridinethiolate complex of Eu(III) would be stable, but the intense color of all these Eu(III) compounds, as well as compound **3**, indicates that LMCT absorptions are relatively low-energy processes. The marginal stability of the trivalent oxidation state in **3** is also consistent with previous reports that suggested Eu(III) is unstable when arenethiolate ligands were the only anions present.^{3k,11}

In contrast to the arenethiolates of Sm, Eu, and Yb, **3** can be handled in air over a period of a day with no apparent decomposition. The isolated crystalline complex is thermally stable because the chelating pyridine donor eliminates the problem of neutral donor ligand dissociation and at the same time maximizes the primary coordination number at the metal center. Compound **3** is also relatively stable in solution. If **3** is dissolved in CH₃CN and the solution is exposed to the atmosphere, the solution remains colored for a period of hours before depositing a white precipitate that will not redissolve. These observations support the conclusion that the pyridinethiolate ligand significantly enhances the stability of ionic complexes in higher oxidation states.

Electronic Spectra. The visible spectra of the redox active Ln(II) chalcogenolates are dominated by fⁿ to fⁿ⁻¹d¹ promotions (Sm, Eu) and MLCT absorptions (Sm, Eu, Yb), if the metal is coordinated to a neutral donor with low-lying acceptor orbitals. The CT absorption has been assigned in related Eu(II) selenolate^{3e} and tellurolate^{3f} studies, where the intense color of the pyridine coordination complexes and the absence of color in the THF coordination complexes led to the conclusion that the color is due to a relatively low-energy Eu(II)-to-pyridine charge transfer (CT) absorption. By analogy, the visible absorption of complex **1** is attributed to an intense but unresolved Eu-to-pyridine charge transfer excitation.

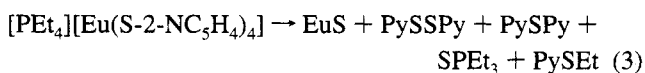
Assignment of the intense visible absorption in **3** as a LMCT band also has considerable precedent in the chalcogenolate chemistry of all three redox active lanthanides Sm, Eu, and Yb. In early Yb work using sterically demanding, highly electronegative ancillary ligands such as Cp* or the heteroallylic ligands, the resultant Yb(III) compounds^{2b-d,g,h} were always intensely colored, although no molar absorptivities were reported. Even samarium, which has the most stable trivalent oxidation state of the redox active lanthanides, still forms intensely colored molecules [(Cp*)₂Sm]₂E [E = S, Se, Te] having visible CT absorptions.^{2f}

When these highly electronegative ancillary ligands are absent, the trivalent chalcogenolate chemistry of the redox active lanthanides becomes severely limited: stable Sm(ER)₃ (E = S and Se, but not Te), Yb(ER)₃ (E = S and Se, but not Te), and Eu(ER)₃ (E = S, R = Py but not Ar) compounds have been reported to date. All of the trivalent examples have an absorption in or near the visible portion of the spectrum which completely obscures the unallowed f–f excitations that are more characteristic of Ln compounds. The LMCT assignment in the Ln compounds that contain only chalcogenolates is based primarily on the intense colors of Yb(EPh)₃ (E = S, Se)^{3m} and the colorless Ho and Tb derivatives. By analogy, the intense color of **3** can be attributed to a S-to-Eu charge transfer absorption which is not resolved in the optical spectrum of **3** in THF, CH₃CN, or pyridine.

Thermolysis Chemistry. The thermolysis of compound **3** was investigated for two reasons. First, it was necessary to establish that pyridinethiolate complexes of the lanthanides would decompose to give lanthanide chalcogenide solids. The thioketone–metal amido resonance description of this molecule could in theory lead to the formation of lanthanide nitrides, rather than sulfides. While pyridinechalcogenolates of Cd^{16ab} and Hg^{16b} have recently been shown to decompose cleanly to give metal selenides, the soft, covalent nature of the bonding in group II metals is vastly different from the bonding of the lanthanide elements, and in principle this difference could lead to the formation of alternative solid state products.

Second, **3** was a potential precursor to Eu₂S₃, a solid state compound that is unstable under conventional high-temperature reaction conditions but might be accessible using the relatively mild reaction conditions associated with molecular thermolysis. An example of unusual thermolysis reactivity is the decomposition of Eu(NCS)₃ in an Ar/CS₂ atmosphere^{17a} to give Eu₃S₄.^{17b} If these or derivatives of these pyridinethiolate molecules are to be used to dope Eu_x into sulfide-based optoelectronic materials, then it is important to establish the identity of the solid state thermolysis products. Thermolysis of lanthanide chalcogenolate precursors generally yields the anticipated solids, with Ln(ER)₂ giving LnE^{3b,h} and Ln(ER)₃ giving Ln₂E₃.^{3c,m} To date, the only exception to this observation is the formation of a metastable mixture^{3m} of HoSe/HoSe₂ from the low-temperature decomposition of (py)₃Ho(SePh)₃. Even in the thermolysis of (py)₃Yb(SePh)₃, a molecule having a lower (λ_{max} = 550 nm) Se-to-Yb CT energy than the LMCT energy found for **3**, Yb₂-Se₃ was the final solid state product and reductive elimination of PhSeSePh was not observed.^{3m} The thermolysis of divalent thiolates has been shown to deliver EuS,¹¹ but thermolysis of the trivalent complex **3** could yield a variety of possible solid state products.

After a sample of **3** sealed in Pyrex under vacuum was slowly heated for a day at 500 °C, X-ray powder diffraction of the final solid state material indicated that EuS¹⁸ was the only crystalline solid state product present (reaction 3), and so



pyridinechalcogenolate complexes of the lanthanide elements

(13) Shannon, R. D. *Acta Crystallogr.* **1976**, A32, 751.

(14) Bradley, D. C.; Ghotra, J. S.; Hart, F. A. *J. Chem. Soc., Dalton Trans.* **1973**, 1021.

(15) Evans, W. J.; Shreeve, J. L.; Ziller, J. W. *Organometallics* **1994**, 13, 731.

(16) (a) Cheng, Y.; Emge, T. J.; Brennan, J. G. *Inorg. Chem.* **1994**, 33, 3711–4. (b) Hursthouse, M. B.; Khan, O.; Mazid, M.; Motevalli, M.; O'Brian, P. *Polyhedron* **1990**, 9, 541.

(17) (a) Grizik, A. A.; Boroduelenko, G. P. *Sov. J. Nonferrous Metals* **1975**, 6, 64. (b) Palazzi, M.; Jaulmes, J. *Solid State Chem.* **1978**, 13, 1153 (JCPDS 32-382).

(18) Nowacki, W. Z. *Kristallogr.* **1938**, 99, 339 (JCPDS 3-684, see also JCPDS 26-1419).

can be viewed as precursors to LnE materials. An NMR analysis of the volatile products indicates the presence of a complex mixture of aromatic products and phosphorus-containing compounds. Dipyridinedisulfide could not be detected in the NMR spectrum, but a GCMS analysis indicated the presence of PySSPy, PySPy, SPEt₃, and PySEt in a 1:8:2:3 ratio. Reductive elimination is clearly observed, and the majority of the resultant disulfide presumably reacts with PEt₃ to form the phosphine sulfide and PySPy.

Conclusions

The pyridinethiolate ligand can be used to prepare crystalline Eu(II) and Eu(III) chalcogenolates. The eight-coordinate divalent complexes are thermally unstable with respect to the dissociation of neutral donor ligands from the metal coordination sphere. The divalent complexes are intensely colored when coordinated to pyridine donor ligands because of a EU-to-pyridine CT absorption, whereas the trivalent complex is colored

due to a visible S-to-Eu charge transfer absorption. Thermolysis of the trivalent molecular precursor to give EuS indicates that the pyridinechalcogenolate complexes of the lanthanide elements are potential LnE doping sources.

Acknowledgment. This work was supported by the National Science Foundation under Grant No. CHE-9204160. We thank Dr. T. Emge for assistance with the single-crystal X-ray diffraction experiments and Jongseong Lee for help collecting the X-ray powder diffraction data.

Supporting Information Available: Powder diffraction pattern of the product from the thermolysis of **3** and tables of crystallographic details and refinement results for **1–3** (25 pages). This material is contained in many libraries on microfiche, immediately follows this article in the microfilm version of the journal, and can be ordered from the ACS; see any current masthead page for ordering information.

IC950322H